Proceedings of the 10th Brazilian Congress of Thermal Sciences and Engineering -- ENCIT 2004
Braz. Soc. of Mechanical Sciences and Engineering -- ABCM, Rio de Janeiro, Brazil, Nov. 29 -- Dec. 03, 2004

Paper CIT04-0347

HELICAL FLOW OF SPTT FLUIDS IN CONCENTRIC ANNULI

Daniel Onofre Cruz
Departamento de Engenharia Mecânica, Universidade Federal do Pará- UFPa, Campus Universitário do Guamá, 66075-900 Belém, Pará, Brasil
e-mail: doac@ufpa.br

Fernando Tavares de Pinho
Centro de Estudos de Fenómenos de Transporte, Departamento de Engenharia Mecânica, Universidade do Minho, Campus de Azurém, 4800-058 Guimarães, Portugal
e-mail: fpinho@dem.uminho.pt

Abstract.*An analytical solution has been derived for the axial flow of Phan-Thien—Tanner (PTT) fluids in concentric annuli with inner cylinder rotation. The simplified form of the PTT model is used with the linear stress coefficient of Phan-Thien (1978), but the nonlinearity of the model couples the axial and tangential flows in a complex way. Expressions are derived for the radial variation of both velocities, as well as for the three shear stresses and the two normal stresses. For engineering purposes expressions are given relating the friction factor and the torque coefficient to the Reynolds number, the Taylor number, a non-dimensional number quantifying elastic effects (* εDe^2 *) and the radius ratio. For axial dominated flows fRe and* C_M *are found to depend only on* εDe^2 *and the radius ratio, but as the strength of rotation increases both coefficients become dependent on the ratio between bulk axial and the inner cylinder tangential velocities (* ξ *)which efficiently compacts the effects of the Reynolds and Taylor numbers.*

Keywords*. Annular flow, PTT fluid, viscoelasticity, swirling flow*

1. Introduction

Annular flows of non-Newtonian fluids are found in a wide variety of applications: from drilling oil and gas wells and well completion operations to industrial processes involving waste fluids, synthetic fibres, foodstuffs and the extrusion of molten plastics as well as in some flows of polymer solutions. This has motivated a wealth of research on annular fllows which has been presented by Escudier et al (2002[a]). Of concern here are mainly previous investigations with viscoelastic fluids in concentric annuli under laminar flow conditions.

The vast majority of non-Newtonian investigations in annular flows concern purely viscous fluids obeying the power law model, and yield stress fluids obeying both the Bingham plastic or the Herschel-Bulkley models. For viscoelastic fluids, investigations on laminar flows are scarcer; one of the first to study viscoelastic concentric annular flows without rotation was Bhatnagar (1963), who used a Rivlin-Eriksen model, but in the presence of suction and injection at the cylinder walls. Dierckes and Schowalter (1966) measured the laminar annular flow of polyisobutelene solutions in the presence of rotating inner walls and showed that symmetry of the flow could be predicted from an inelastic theory based on a power law fitted to the experimental rheological data. Kaloni (1965) and Kulshrestha (1962) derived analytical solutions for viscoelastic fluid obeying Oldroyd's equations while Pinho and Oliveira (2000) solved analytically the concentric annular laminar flow without inner cylinder rotation for the simplified PTT model. That work is the immediate predecessor of the present investigation since the adopted rheological constitutive equation is the same, but now the objective is the investigation of the annular flow of the PTT fluid with inner cylinder rotation.

Other analytical studies of swirling viscoelastic flows have been motivated by applications in rheology and tribology, as listed in Cruz and Pinho (2004).

The paper is organised as follows: in the next section the relevant equations are presented, the various non-dimensional numbers are defined and the analytical solution is derived. Plots of relevant quantities are made and discussed in Section 3 and a summary of the main conclusions closes the paper.

2. Governing equations and analytical solution

The flow geometry is a concentric annulus of inner and outer radius R_I and R_O, respectively, defining an annular gap, $\delta \equiv R_O - R_I$, and radius ratio, $\kappa \equiv R_I / R_O$. The flow is fully-developed, and so both the axial velocity, *u*, and the tangential velocity, *v*, are only functions of the radial coordinate *r*; the axial pressure gradient is constant and the inner cylinder is rotating at constant angular velocity, ω. Under these conditions the momentum equations in the axial, *z*, tangential, θ, and radial, *r*, directions are

$$\frac{1}{r}\frac{d}{dr}\left(r\tau_{rz}\right)-\frac{\partial p}{\partial z}=0\,;\; -\rho\frac{v^2}{r}=\frac{1}{r}\frac{d}{dr}\left(r\tau_{rr}\right)-\frac{\tau_{\theta\theta}}{r}-\frac{\partial p}{\partial r}\,;\;\; \frac{d}{dr}\left(r^2\tau_{r\theta}\right)=0 \qquad (1\text{ a,b,c})$$

The extra stresses are given by the simplified form of the PTT constitutive equation (Phan-Thien and Tanner, 1977)

$$f\left(tr(\tau)\right)\tau+\lambda\overset{\nabla}{\tau}=2\eta\boldsymbol{D}\ \text{ with }\ f\left(tr(\tau)\right)=1+\frac{\varepsilon\lambda}{\eta}tr(\tau) \qquad (2)$$

where $\boldsymbol{D}$ is the deformation rate tensor, λ is the relaxation time, η is the viscosity coefficient and ε is a parameter of the model limiting the extensional viscosity of the fluid. The stress coefficient function $f\left(tr(\tau)\right)$, defined in Eq. (2), is the linearization of the more general exponential coefficient and $\overset{\nabla}{\tau}$ denotes Oldroyd's upper convective derivative $\overset{\nabla}{\tau}=\frac{D\tau}{Dt}-\tau.\nabla\boldsymbol{u}-(\nabla\boldsymbol{u})^T.\tau$. For this flow geometry the constitutive equation simplifies to

$$\tau_{rr}=0\,;\;\tau_{zz}=\frac{2\lambda\eta}{f(\tau_{ii})^2}\left(\frac{du}{dr}\right)^2;\;\tau_{\theta\theta}=\frac{2\lambda\eta}{f(\tau_{ii})^2}\left[r\frac{d}{dr}\left(\frac{v}{r}\right)\right]^2 \qquad (3\text{ a,b,c})$$

$$\tau_{r\theta}=\frac{\eta r}{f(\tau_{ii})}\frac{d}{dr}\left(\frac{v}{r}\right);\;\tau_{rz}=\frac{\eta}{f(\tau_{ii})}\frac{du}{dr};\;\tau_{\theta z}=\frac{2\lambda\eta r}{f(\tau_{ii})^2}\frac{du}{dr}\frac{d}{dr}\left(\frac{v}{r}\right) \qquad (4\text{ a,b,c})$$

where the stress coefficient $f(\tau_{ii})$ was used for compactness. The stress coefficient is now given by the following non-linear cubic equation

$$f(\tau_{ii})=1+\frac{2\varepsilon\lambda^2}{f(\tau_{ii})^2}\left[\left(\frac{du}{dr}\right)^2+\left(r\frac{d}{dr}\left(\frac{v}{r}\right)\right)^2\right] \qquad (5)$$

The boundary conditions for this problem express no-slip at the walls: $r=R_I\Rightarrow u=0, v=\omega R_I$ and $r=R_O\Rightarrow u=0, v=0$. Introducing the torque per unit length of the cylinder (M), integration of Eq. (1-c) gives the variation of one stress component: $\tau_{r\theta}=M/\left(2\pi r^2\right)$. Substituting this result into Eq. (4-a) provides the following expression

$$r\frac{d}{dr}\left(\frac{v}{r}\right)=\frac{M}{2\pi\eta r^2}f(\tau_{ii}) \qquad (6)$$

that can be used to calculate $\tau_{\theta\theta}$ in Eq. (3-c), giving the result $\tau_{\theta\theta}=\lambda M^2/\left(2\pi^2\eta r^4\right)$.

Now, using this stress into the radial momentum equation (Eq. 1-b) gives

$$r\frac{\partial p}{\partial r}=\rho v^2-\frac{\lambda M^2}{2\pi^2\eta r^4} \qquad (7)$$

which provides the radial distribution of pressure once the radial variation of the tangential velocity is known.

To obtain the axial velocity it is still necessary to deduce expressions for τ_{rz} and τ_{zz}, that depend only on derivatives of velocity and pressure. Eq. (1-a) can be integrated into

$$\tau_{rz}=\frac{\partial p}{\partial z}\frac{r}{2}+\frac{c_2}{r} \qquad (8)$$

where c_2 is an integration constant. With τ_{rz} also given by Eq. (4-b), the stress coefficient function is determined as

$$f(\tau_{ii})=\frac{\eta\frac{du}{dr}}{\frac{\partial p}{\partial z}\frac{r}{2}+\frac{c_2}{r}} \qquad (9)$$

Squaring this function and using it in Eq. (3-b) leads to

$$\tau_{zz} = \frac{2\lambda}{\eta}\left[\frac{\partial p}{\partial z}\frac{r}{2} + \frac{c_2}{r}\right]^2 \tag{10}$$

Now, it is possible to determine the axial and tangential velocity profiles. According to Eq. (9), the definition of $f(\tau_{ii})$ and after substitution of $\tau_{\theta\theta}$ and using Eq. (10), the following axial velocity gradient is deduced

$$\frac{du}{dr} = \frac{1}{\eta}\left[\frac{\partial p}{\partial z}\frac{r}{2} + \frac{c_2}{r}\right] + \frac{2\lambda^2\varepsilon}{\eta^3}\left[\frac{\partial p}{\partial z}\frac{r}{2} + \frac{c_2}{r}\right]\left\{\frac{M^2}{4\pi^2 r^4} + \left[\frac{\partial p}{\partial z}\frac{r}{2} + \frac{c_2}{r}\right]^2\right\} \tag{11}$$

A solution in terms of non-dimensional quantities is sought. For simplicity and prior to integration, the following characteristic parameters are defined: an axial velocity scale $U_c = -p_{,z}\delta^2/(8\eta)$, a tangential velocity scale $U_T = M/(\pi\eta\delta)$, and the corresponding characteristic Deborah numbers $De_c = \lambda U_c/\delta$ and $De_T = \lambda U_T/\delta$. Alternative Deborah numbers are defined on the basis of the axial bulk velocity (U leading to $De \equiv \lambda U/\delta$) and of the tangential velocity of the inner cylinder ($U_{T_i} = \omega R_I$ leading to $De_{T_i} = \lambda U_{T_i}/\delta$).

Five independent non-dimensional quantities are needed to fully characterise the flow: ε and a Deborah number related to the axial flow (*De* or De_c) are constitutive parameters, the radius ratio κ is a geometric parameter, and the rotating Deborah number (De_T or De_{T_i}), or alternatively a Taylor number or a rotational Reynolds number, and the axial flow Reynolds number (*Re*), all of which are dynamical parameters. The axial Reynolds number is defined as $Re = 2\delta\rho U/\eta$, i.e., it is based on the hydraulic diameter $D_H = 4A/P = 2\delta$, where *A* is the cross section area and *P* is the corresponding wetted perimeter. Elsewhere, δ was used as the length scale.

After normalisation and integration of Eq. (11), the axial velocity profile u/U is given by

$$\begin{aligned}\frac{u}{U} = &-2\frac{U_c}{U}y^2 - 4\tilde{c}_2\frac{U_c}{U}\ln y + \frac{\varepsilon De_T^2}{y^2}\frac{U_c}{U} + \frac{\varepsilon De_T^2}{2}\frac{U_c}{U}\frac{\tilde{c}_2}{y^4} - 32\varepsilon De_c^2\frac{U_c}{U}y^4 - 192\varepsilon De_c^2\frac{U_c}{U}\tilde{c}_2 y^2 \\ &-384\varepsilon De_c^2\frac{U_c}{U}\tilde{c}_2^2\ln y + 64\varepsilon De_c^2\frac{U_c}{U}\frac{\tilde{c}_2^3}{y^2} + \tilde{c}_3\end{aligned} \tag{12}$$

where the radial coordinate is presented in normalised form as $y = r/\delta$.

In Eq. (12) the new constant of integration c_3 and constant c_2 appear in normalized form: $\tilde{c}_2 \equiv 2c_2/p_{,z}\delta^2$ and $\tilde{c}_3 \equiv c_3/U$. From Eq. (6), and using the stresses $\tau_{\theta\theta}$ and τ_{zz}, the differential equation for the tangential velocity is obtained. After normalisation and integration, the following tangential velocity profile is obtained:

$$\frac{v}{U} = -\frac{1}{4y}\frac{U_T}{U} - \frac{1}{24y^5}\varepsilon De_T^2\frac{U_T}{U} + 16\varepsilon De_c^2\frac{U_T}{U}y\ln y - 16\varepsilon De_c^2\frac{U_T}{U}\frac{\tilde{c}_2}{y} - 4\varepsilon De_c^2\frac{U_T}{U}\frac{\tilde{c}_2^2}{y^3} + \tilde{c}_4 y \tag{13}$$

The new nondimensional constant of integration is $\tilde{c}_4 = c_4\delta/U$.

Application of the boundary conditions to the velocity profiles provides equations to determine the constants of integration. No-slip condition of the axial velocity at both walls (Eq. 12) gives the following cubic equation on $\tilde{c}_2$

$$b_0 + b_1\tilde{c}_2 + b_2\tilde{c}_2^2 + b_3\tilde{c}_2^3 = 0 \tag{14}$$

with coefficients

$$\begin{aligned}&b_0 = 2\left(y_o^2 - y_i^2\right) + \varepsilon De_T^2\left(\frac{1}{y_i^2} - \frac{1}{y_o^2}\right) + 32\varepsilon De_c^2\left(y_o^4 - y_i^4\right);\ b_1 = 4\ln\frac{y_o}{y_i} - \frac{\varepsilon De_T^2}{2}\left(\frac{1}{y_o^4} - \frac{1}{y_i^4}\right) + 192\varepsilon De_c^2\left(y_o^2 - y_i^2\right) \\ &b_2 = 384\varepsilon De_c^2\ln\frac{y_o}{y_i};\ b_3 = -64\varepsilon De_c^2\left(\frac{1}{y_o^2} - \frac{1}{y_i^2}\right)\end{aligned} \tag{15}$$

This cubic equation has the following solution

$$\tilde{c}_2 = \mathrm{sign}(p)|p|^{1/3} + \mathrm{sign}(q)|q|^{1/3} - \frac{a_1}{3} \qquad \text{with}$$

$$p = -\frac{b}{2} + \sqrt{d}\,;\; q = -\frac{b}{2} - \sqrt{d}\,;\; d = \frac{b^2}{4} + \frac{a^3}{27}\,;\; a = a_2 - \frac{a_1^2}{3}\,;\; b = a_3 - \frac{a_1 a_2}{3} + \frac{2a_1^3}{27}\,;\; a_1 = \frac{b_2}{b_3}\,;\; a_2 = \frac{b_1}{b_3}\,;\; a_3 = \frac{b_0}{b_3} \quad (16)$$

Once $\tilde{c}_2$ is known, determination of the other two constants is straightforward: $\tilde{c}_3$ is obtained from Eq. (12) by setting the no-slip condition at any of the walls and $\tilde{c}_4$ is calculated with Eq. (13) applying the no-slip condition at the outer wall. The axial bulk velocity is calculated from its definition for an annulus and is given by

$$U = \frac{2(1-\kappa)}{1+\kappa}\int_{y_i}^{y_o} u y\,dy = \frac{2(1-\kappa)}{1+\kappa}\left[-\frac{1}{2}U_c\left(y_o^4 - y_i^4\right) - 2\tilde{c}_2 U_c\left(\frac{y_i^2}{2} - \frac{y_o^2}{2} + y_o^2 \ln y_o - y_i^2 \ln y_i\right) + \varepsilon De_T^2 U_c \ln\frac{y_o}{y_i} - \right.$$
$$\frac{\varepsilon De_T^2}{4} U_c \tilde{c}_2\left(\frac{1}{y_o^2} - \frac{1}{y_i^2}\right) - \frac{16}{3}\varepsilon De_c^2 U_c\left(y_o^6 - y_i^6\right) - 48\varepsilon De_c^2 U_c \tilde{c}_2\left(y_o^4 - y_i^4\right) +$$
$$\left. 192\varepsilon De_c^2 U_c \tilde{c}_2^2\left(\frac{y_i^2}{2} - \frac{y_o^2}{2} + y_o^2 \ln y_o - y_i^2 \ln y_i\right) + 64\varepsilon De_c^2 U_c \tilde{c}_2^3 \ln\frac{1}{\kappa} + \frac{\tilde{c}_3}{2}\left(y_o^2 - y_i^2\right) = \right] \quad (17)$$

Setting $v = \omega y_i \delta$ at $y = y_i$ in Eq. (13) gives the angular rotational speed

$$\omega = \frac{1}{y_i \delta}\left[-\frac{U_T}{4y_i} - \frac{\varepsilon De_T^2}{24}\frac{U_T}{y_i^5} + 16U_T \varepsilon De_c^2 y_i \ln y_i - 16U_T \varepsilon De_c^2 y_i \ln y_i \frac{\tilde{c}_2}{y_i} - 4U_T \varepsilon De_c^2 \frac{\tilde{c}_2^2}{y_i^3} + \delta \tilde{c}_4 y_i\right] \quad (18)$$

The stress field can also be presented in nondimensional form using the various non-dimensional parameters presented. Note the different velocity scales used to normalise axial related and rotation related stress tensor components.

$$T_{rz} \equiv \frac{\tau_{rz}}{\eta\frac{U_c}{\delta}} = -4\left(y + \frac{\tilde{c}_2}{y}\right);\; T_{r\theta} \equiv \frac{\tau_{r\theta}}{\eta\frac{U_T}{\delta}} = \frac{1}{2y^2};\; T_{zz} \equiv \frac{\tau_{zz}}{\eta\frac{U_c}{\delta}} = 2De_c T_{rz}^2 = 32De_c\left(y + \frac{\tilde{c}_2}{y}\right)^2$$
$$T_{\theta\theta} \equiv \frac{\tau_{\theta\theta}}{\eta\frac{U_T}{\delta}} = 2De_T T_{r\theta}^2 = \frac{De_T}{2y^4};\; T_{\theta z} \equiv \frac{\tau_{\theta z}}{\eta\frac{U_T}{\delta}} = 2De_c T_{r\theta} T_{rz} = -\frac{4De_c}{y^2}\left[y + \frac{\tilde{c}_2}{y}\right] \quad (19\text{ a,b,c,d,e})$$

The axial pressure gradient is more conveniently written as the Fanning friction factor *f* and, as shown in Pinho and Oliveira (2000), in the case of the PTT model it is given by

$$f\,\mathrm{Re} = 16\frac{U_c}{U} \quad (20)$$

which can be compared with the corresponding expression for Newtonian fluids

$$(f\,\mathrm{Re})_N = 16\frac{1}{(1+\kappa)^2/(1-\kappa)^2 - (1+\kappa)/(1-\kappa)\left(1/\ln(1/\kappa)\right)} \quad (21)$$

The torque required to rotate the inner cylinder is quantified as a torque coefficient C_M defined so that it is unity for Newtonian fluids (*M* is torque per unit length).

$$C_M \equiv \frac{M\left(R_o^2 - R_i^2\right)}{4\pi\omega\eta R_o^2 R_i^2} \quad (22)$$

For this flow, it can be shown that C_M is given by

$$C_M = \frac{U_T}{U_{T_i}} \frac{\left(1-\kappa^2\right)(1-\kappa)}{4\kappa} \tag{23}$$

Finally, to quantify the rotation it is usual to use either the rotational Reynolds number (T) or, alternatively, the Taylor number (Ta)

$$T = \frac{\rho\omega R_I \delta}{\eta};\ Ta = \left(\frac{\rho\omega}{\eta}\right)^2 R_I \delta^3 \tag{24 a,b}$$

which are related to each other, and to De_{T_i}, as below

$$T = \frac{Re}{2De} De_{T_i};\ Ta = \left(\frac{1}{\kappa}-1\right) T^2 = \left(\frac{1}{\kappa}-1\right)\left(\frac{Re}{2De}\right)^2 De_{T_i}^2 \tag{25 a,b}$$

The combination of Re, De and De_{T_i} into those more typical nondimensional numbers, makes them more difficult to use analytically.

3. Results and discussion

The presentation of results is divided into two parts. First, radial profiles of velocity and stress components are shown to illustrate the influence of the various relevant non-dimensional numbers. In the second part, results of more engineering interest are presented for the direct and indirect problems.

3.1. Detailed flow characteristics

In the absence of inner cylinder rotation ($Ta = 0$) our solution matches that of Pinho and Oliveira (2000), but this is not shown here. For inelastic fluids, Escudier et al (2002 a) identified three different flow regimes, according to the relative strengths of axial and tangential flow ($\xi \equiv \omega R_I / U$). If $\xi < 1$, the flow is dominated by the axial flow, for $\xi > 10$ rotation dominates and a mixed flow conditions prevail elsewhere.

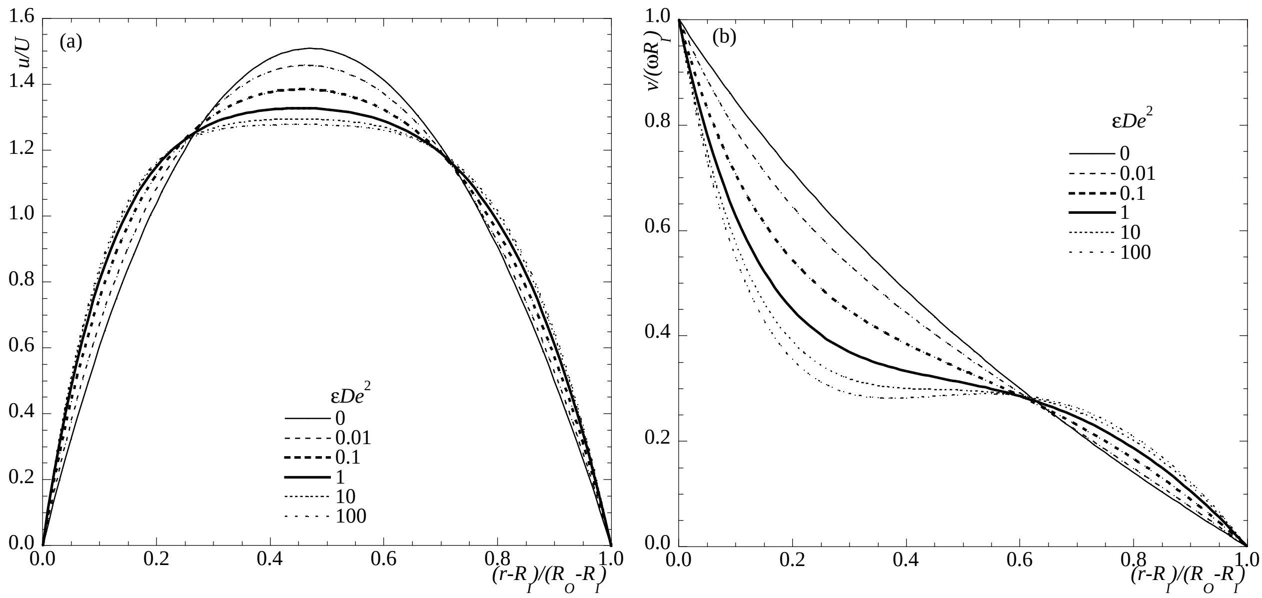

Figure 1. Radial profiles of the normalised axial (a) and tangential (b) velocities in an annulus of κ = 0.5 for an SPTT fluid for axial-dominated flow conditions (*Re*= 1,000; *Ta*= 1,000).

The axial and tangential velocity profiles presented in Figures 1 to 2 pertain to the two limiting flow regimes. In the axially-dominated flow regime, the variation of the axial velocity profile in Figure 1-a) is like that for no cylinder rotation in Pinho and Oliveira (2000), with flow elasticity (εDe^2) imparting a plug-like shape. In terms of tangential velocity, the flow elasticity parameter also has a dramatic influence as can be seen in Figure 1-b). As εDe^2 increases the $v/(\omega R_I)$ profile becomes increasingly distorted to a sigmoidal shape and for εDe^2 in excess of about 10 the profile is no longer monotonic. This behaviour is akin to that seen by Nouar et al (1998), and also calculated by Escudier et al (2002b), and is due to the intense shear-thinning of the viscometric viscosity of the fluids. For lower Taylor numbers, leading to ξ below the present value of 0.006325, the same patterns are observed.

For rotation-dominated flow Figure 2 plots the axial and tangential velocity profiles corresponding to a condition with $\xi = 200$. To understand the observed variations it is important to realise that, whereas in axially dominated flow the shear-thinning behaviour affects the whole annular space, here the high rates of deformation and the shear-thinning behaviour concentrate near the inner cylinder. Higher values of *Ta* would increase the extent of such region, but this would correspond to conditions where laminar flow becomes unstable. In fact, for Taylor numbers in excess of 50,000 secondary flows are known to appear due to flow instabilities. For the concentric geometry, and in the absence of any elasticity, the PTT model simplifies to the Newtonian behaviour for which there is a perfect decoupling between axial and tangential flows.

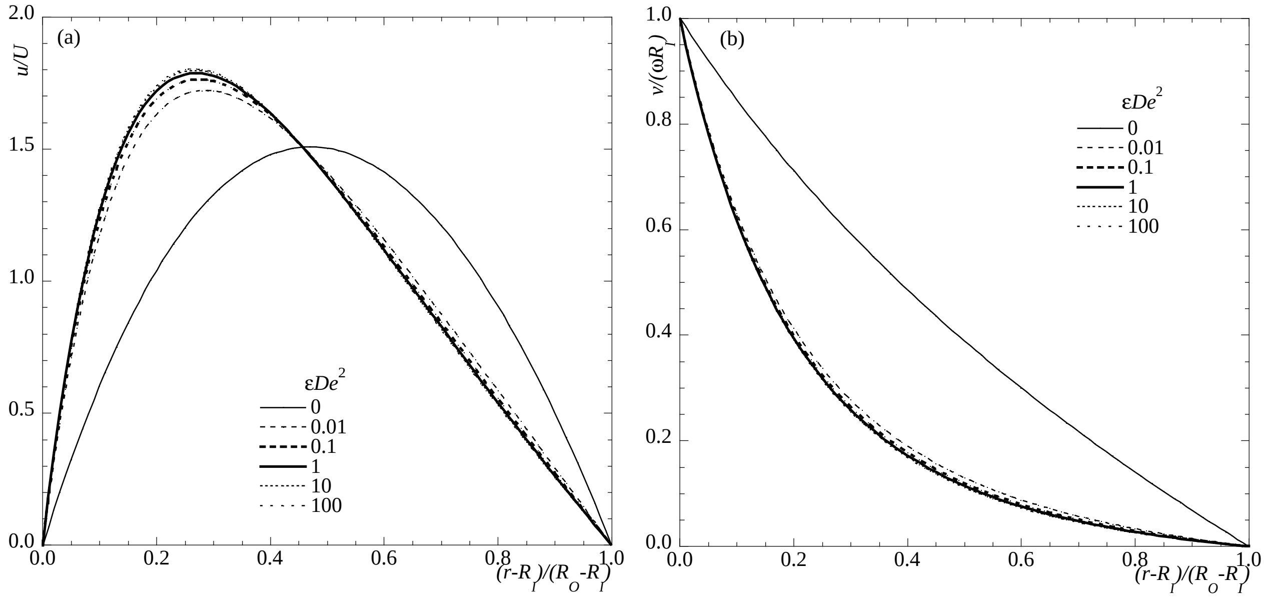

Figure 2. Radial profiles of the normalised axial (a) and tangential (b) velocities in an annulus of κ = 0.5 for an SPTT fluid for rotation-dominated flow conditions (*Re*= 1; *Ta*= 10,000).

As soon as εDe^2 differs from zero both flows are coupled and the axial flow becomes highly distorted towards the inner cylinder and the peak velocities increase around 15% because of the lower viscosities there. Similarly, for the tangential velocity in Figure 2-b) a strong deviation of the flow towards the inner cylinder is seen. The effect of the Deborah number is also weaker than for $\xi < 1$, because now (for $\xi > 10$) the rates of deformation of the fluid are weaker. Still, a tendency is observed for the maximum axial velocity to decrease and for the profile to widen as εDe^2 increases.

Under the mixed flow conditions, not shown here, the axial and tangential velocity profiles show better the progression from the Newtonian decoupled flow to the flow dominated by elasticity as εDe^2 increases.

The radial variation of the various stress tensor components is analysed in detail. In Figure 3-a) the shear stress due to rotation ($\tau_{r\theta}$) is plotted in normalised form and is seen to have a universal form regardless of the values of *Re*, *Ta* and εDe^2. This is immediately clear from inspection of its definition in Eq. (21-b). In contrast, the definition of the axial shear stress in Eq. (21-a) shows this component not to be independent of *Re*, *Ta* and εDe^2 via the constant of integration $\tilde{c}_2$ and Figure 3 also shows its variation, including a set pertaining to the mixed flow regime. For a Newtonian fluid, or in the absence of rotation, T_{rz} is independent of flow elasticity and balances the axial pressure gradient as is known from Pinho and Oliveira (2000). For an axial-dominated flow there is a weak dependence of T_{rz} on εDe^2, because of the decrease in viscosity due to the rotational flow and this is seen in Figure 3-a). The dependence on εDe^2 is clearer in Figure 3-b) which shows the progression of T_{rz} from an independent profile at εDe^2=0 towards the profile for a rotation dominated flow. When the flow is dominated by rotation (curves for *Ta*=10000), the viscosity is basically defined by the rotational flow and the weak dependence of T_{rz} on εDe^2 is due to the slight effect of the axial flow upon the viscosity. Under mixed flow conditions (curves for *Ta*=10), the viscosity is strongly affected by both the axial and the rotational flow and now the variation of T_{rz} with εDe^2 is stronger, reflecting the changes in viscosity across the annulus. T_{rz} is proportional to the axial velocity gradient hence in axial dominated flows T_{rz} goes to zero near the center of the annulus where the peak velocity occurs. Since rotation deviates the axial flow towards the inner wall, T_{rz} decreases here and increases in the outer wall region as is well shown.

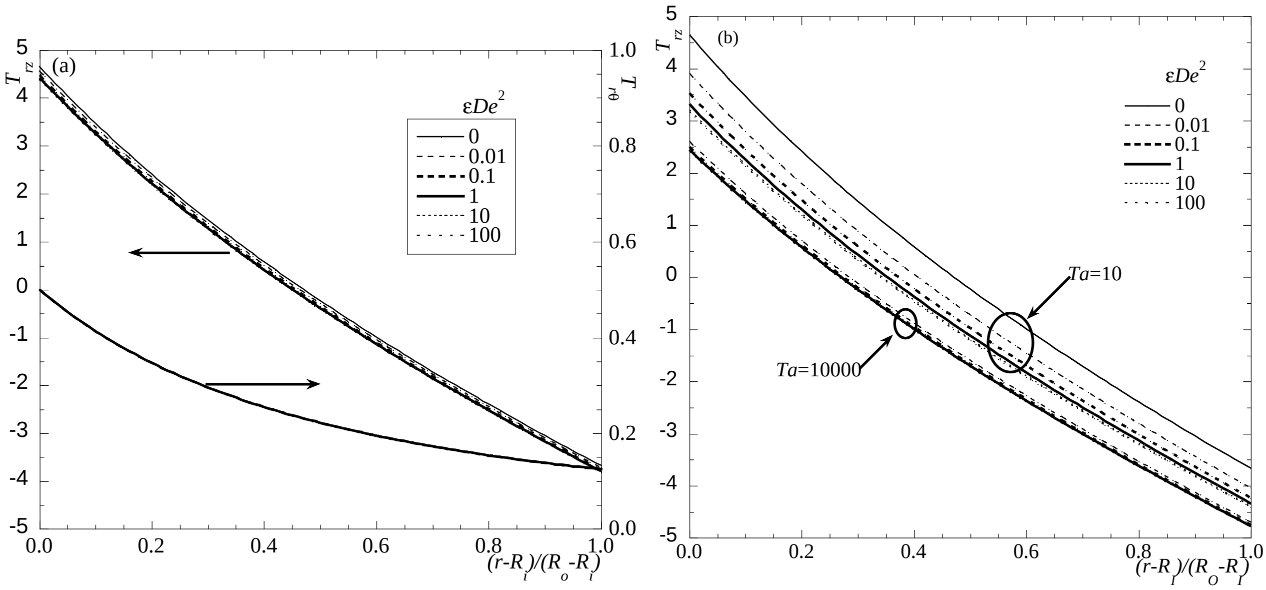

Figure 3. Radial profiles of the nondimensional shear stresses τ_{rz} and $\tau_{\theta r}$ for an SPTT fluid in annuli with κ = 0.5.: a) *Re*= 1,000, *Ta*=10,000 ($\xi = 0.2$); b) *Re*=1 with *Ta*= 10 ($\xi = 6.325$) and *Ta*= 10,000 ($\xi = 200$).

Due to the combined axial and rotational flows, the tangential axial shear stress $\tau_{\theta z}$ is non-zero and varies with elasticity, *Re* and *Ta*. Since this stress can be normalised in two different ways (c.f. Eq. 19-e) the magnitude of the radial variations depends on the normalisation and also on ξ. These are not shown here due to space limitations, but a more thorough investigation is found in Cruz and Pinho (2004).

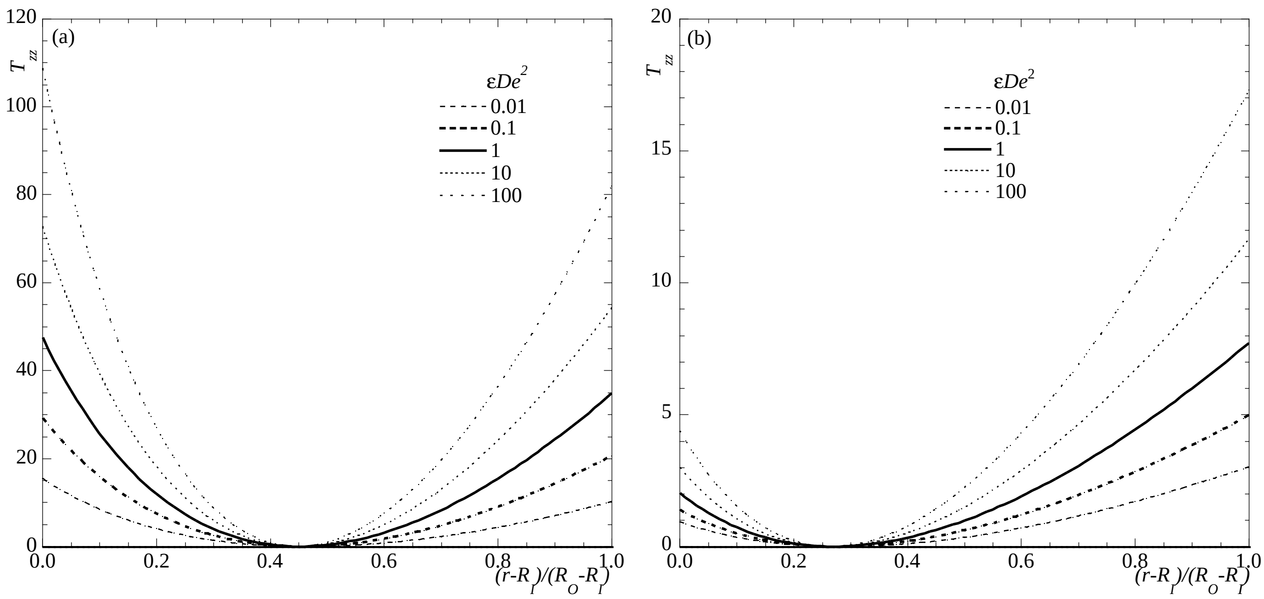

Figure 4. Radial profiles of the nondimensional T_{zz} normal stress of an SPTT fluid in annuli with κ = 0.5: a) *Re*= 1,000, *Ta*= 10,000; b) *Re*= 1, *Ta*= 10,000.

The axial normal stress variations are shown in Figure 4. These are exclusively due to the strength of the axial flow, via its radial gradient squared, and fluid elasticity, but are also affected by rotation (c.f. Eq. 21-c) due to the distortions in the axial flow. For axially dominated flows, Figure 4-a), the stresses increase with flow elasticity and reach maxima of the order of 100 for εDe^2=100. As rotation increases in strength, the curves move towards the inner cylinder and the magnitude of the stresses decrease significantly as can be seen in Figure 4-b); note the different ordinates in Figures 4-

a) and -b) showing a decrease by a factor of 6. As mentioned above, this reduction is due to lower rates of deformation in the rotation dominated flows.

Finally, for the tangential normal stress the behaviour is qualitatively opposite to that of the axial normal stress. $T_{\theta\theta}$ is due to the rotational flow, via the radial gradient of the tangential velocity squared, and fluid elasticity. The effect of the axial flow is more difficult to observe given the monotonic variation of the tangential velocity. Profiles of $T_{\theta\theta}$ are plotted in Figure 5-a) and 5-b) for axially dominated and rotation dominated flows, respectively. Note the different ordinates in the figures showing values of $T_{\theta\theta}$ in the axially dominated case that are 40 times smaller than in Figure 5-b).

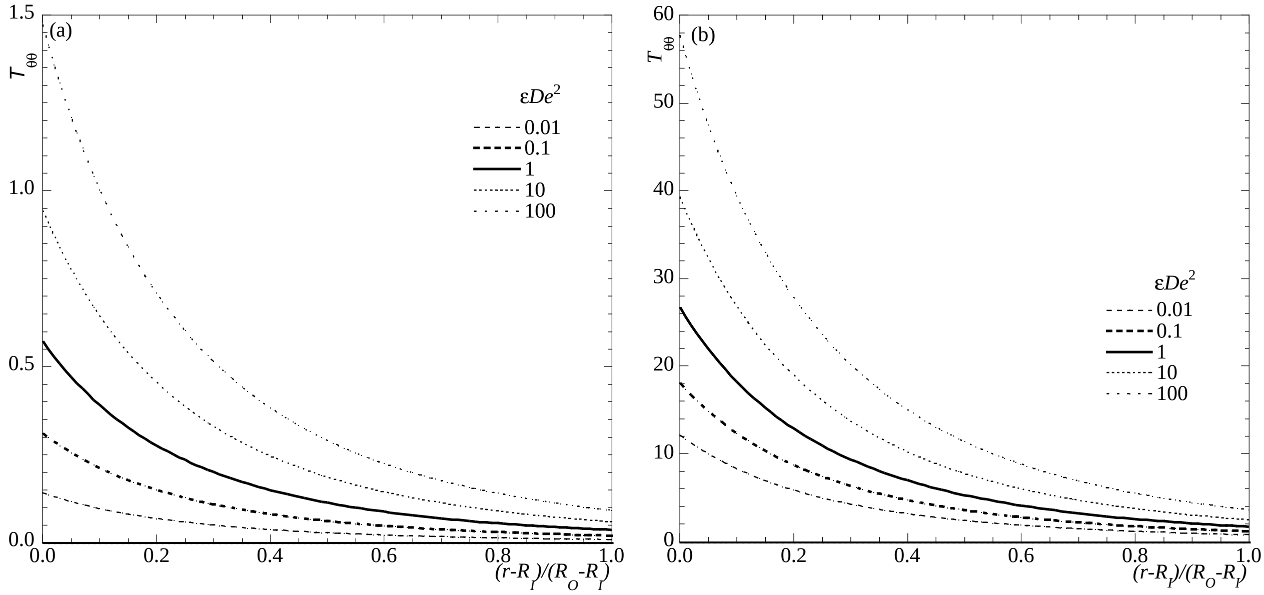

Figure 5. Radial profiles of the nondimensional $T_{\theta\theta}$ normal stress of an SPTT fluid in annuli with κ = 0.5: a) *Re*= 1,000, *Ta*= 10,000; b) *Re*= 1, *Ta*= 10,000.

3.2. Bulk flow characteristics

In analysing the bulk flow characteristics the main concern is to possess expressions that allow the resolution of the so-called direct and indirect problems, via universal relations that are based on non-dimensional quantities. All the equations relating the relevant quantities have already been presented in Section 2 and here the focus is on defining the correct sequence of the calculations and in plotting the corresponding results as a function of the more useful Reynolds number of the axial flow, Taylor number and εDe^2.

In the direct problem the Reynolds number (or the axial bulk velocity) and the Taylor number (or rotational speed) are known quantities and we wish to determine the friction factor (or the pressure gradient) and the torque coefficient (or the torque). The product fRe is given by Eq. (20) and requires knowledge of the ratio U_c/U whereas C_M, defined in Eq. (21), needs the ratio U_T/U_{T_i}. Due to the non-linear characteristics of the PTT fluid, fRe and C_M are not decoupled quantities since U_c/U depends on U_T/U_{T_i} and vice-versa, as can be seen below.

To obtain these velocity ratios it is necessary to solve a system of three non-linear equations that result from the application of boundary conditions to Eqs. (12) and (13) for the axial and tangential velocities, respectively, and the calculation of the axial bulk velocity via Eq. (19). The first relation is the cubic equation (14) to determine $\tilde{c}_2$, which affects both U_c/U and U_T/U_{T_i} and, the quadratic equations (26) and (27) to determine the ratios U_c/U and U_T/U_{T_i}, respectively. Although Eq. (27) is quadratic on U_T/U_{T_i}, its determination is straighforward.

$$-\frac{1}{4}\frac{U_T}{U_{T_i}}\left(\frac{1}{y_i}-\frac{y_i}{y_o^2}\right)-\frac{\varepsilon De_{T_i}^2}{24}\left(\frac{U_T}{U_{T_i}}\right)^3\left(\frac{1}{y_i^5}-\frac{1}{y_o^6}\right)+16\varepsilon De^2\frac{U_T}{U_{T_i}}\left(\frac{U_c}{U}\right)^2 y_i\ln\kappa-$$
$$16\varepsilon De^2\frac{U_T}{U_{T_i}}\left(\frac{U_c}{U}\right)^2\tilde{c}_2\left(\frac{1}{y_i}-\frac{y_i}{y_o^2}\right)-4\varepsilon De^2\frac{U_T}{U_{T_i}}\left(\frac{U_c}{U}\right)^2\tilde{c}_2^2\left(\frac{1}{y_i^3}-\frac{y_i}{y_o^4}\right)=1 \qquad (26)$$

$$-\frac{1}{2}\frac{U_c}{U}\left(y_o^4-y_i^4\right)-2\tilde{c}_2\frac{U_c}{U}\left(\frac{y_i^2}{2}-\frac{y_o^2}{2}+y_o^2\ln y_o-y_i^2\ln y_i\right)+\varepsilon De_{T_i}^2\left(\frac{U_T}{U_{T_i}}\right)^2\frac{U_c}{U}\ln\frac{y_o}{y_i}-$$
$$\frac{\varepsilon De_{T_i}^2}{4}\left(\frac{U_T}{U_{T_i}}\right)^2\frac{U_c}{U}\tilde{c}_2\left(\frac{1}{y_o^2}-\frac{1}{y_i^2}\right)-\frac{16}{3}\varepsilon De^2\left(\frac{U_c}{U}\right)^3\left(y_o^6-y_i^6\right)-48\varepsilon De^2\left(\frac{U_c}{U}\right)^3\tilde{c}_2\left(y_o^4-y_i^4\right)+$$
$$192\varepsilon De^2\left(\frac{U_c}{U}\right)^3\tilde{c}_2^2\left(\frac{y_i^2}{2}-\frac{y_o^2}{2}+y_o^2\ln y_o-y_i^2\ln y_i\right)+64\varepsilon De^2\left(\frac{U_c}{U}\right)^3\tilde{c}_2^3\ln\frac{1}{\kappa}+\frac{\tilde{c}_3}{2}\left(y_o^2-y_i^2\right)=\frac{1+\kappa}{2(1-\kappa)} \tag{27}$$

In the indirect problem, the friction factor and torque coefficient are known quantities and the aim is to determine the Reynolds and the Taylor numbers. In this case the solution is straightforward. To determine the bulk velocity and angular speed it suffices to use Eqs. (17) and (18), respectively and the definitions of the characteristic velocities U_c and U_T. Then *Re* and *Ta* can be calculated using their definitions.

The variations of fRe and C_M with *Re*, *Ta* and εDe^2 for κ = 0.5 are shown in Figures 6-a) and 6-b), respectively. It was found that the relevant independent quantities that determine fRe and C_M are just εDe^2 and the velocity ratio ξ, the latter compacting the effects of both *Re* and *Ta* according to its definition ($\xi \equiv 2T/Re$). For axially dominated flows ($\xi < 1$) *fRe* and C_M only depends on εDe^2 as represented in Figures 6-a) and 6-b) by the curves for $\xi \le 0.2$. The effect of εDe^2 is to reduce both *fRe* and C_M because the fluid becomes more shear-thinning thus reducing the viscosity near the walls. The universal behaviour of C_M is due to the fact that viscosity is defined by the axial flow and is independent of the magnitude of rotation in this flow regime. Note also that the definition of C_M is such that it is always bounded by 1 in the Newtonian limit.

With increased rotation, the *fRe* versus εDe^2 curves are shifted to the left showing a decrease in friction factor for the axial flow because of the decreased viscosity imparted to the shear-thinning fluid by the increasingly strong rotation. As rotation comes to dominate the flow, the axial flow no longer determines the shear-thinning viscosity. The energy loss decreases for both axial and tangential flow and so the normalised resistance coefficients *fRe* and C_M decrease at identical values of the elasticity parameter εDe^2.

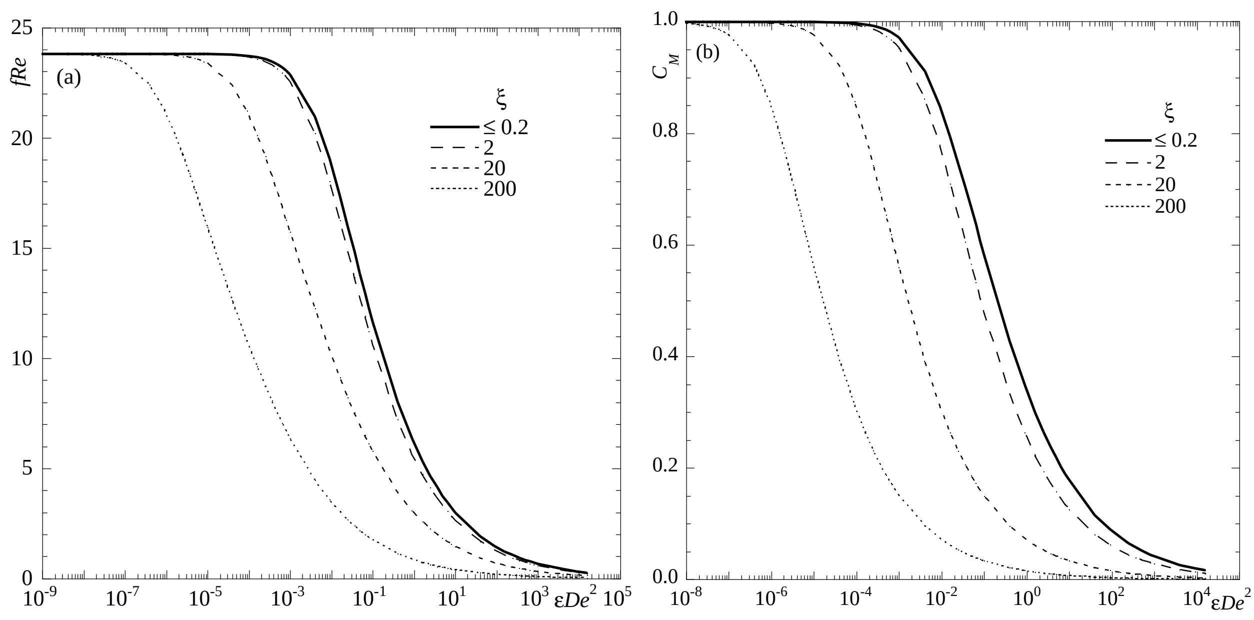

Figure 6. Variation of *fRe* (a) and C_M (b) with ξ and εDe^2 of an SPTT fluid in annuli with κ = 0.5.

Although these effects take place for an elastic fluid, they are due to the inherent shear-thinning behaviour of the SPTT fluid and, consequently, the conclusions regarding C_M and *fRe* are in agreement with the observations of Escudier et al (2002a) for inelastic power law fluids in concentric annuli.

4. Conclusions

An analytical solution has been deduced for the helical flow of single-mode viscoelastic PTT fluids in concentric annuli. This flow is formed by the combination of an imposed constant axial pressure gradient with rotation of the inner cylinder. Expressions in normalized form are presented for the axial and tangential velocities, all stress components and for the friction factor and torque coefficients.

Under conditions of axial-dominated flow the peak axial velocity is in the center of the annulus and becomes plug like as εDe^2 increases, while the tangential velocity progressively distorts to a sigmoidal shape. The tangential shear stress, that balances the applied torque, has always a universal behaviour and the axial shear stress, balancing the axial pressure gradient, has quasi-universal variation with εDe^2. In contrast, for rotation dominated flows the tangential velocities always have a monotonic variation and the flow is distorted towards the inner cylinder where viscosities are lower.

For the bulk flow characteristics, *fRe* and C_M only depend on εDe^2 for a given annulus when flow is axially dominated, but they decrease with the velocity ratio (ξ) as rotation increases in strength. In all cases, an increase in εDe^2 leads to reduce resistance in the axial and rotational flow. It was also found that ξ adequately compacts the effects of *Re* and *Ta* on *f* and C_M .

5. Acknowledgements

The authors wish to thank CNPq of Brazil and ICCTI of Portugal for funding this work via the exchange programme Project 2001 Proc C 4.3.1 in 2002.

6. References

Alves MM, Pinho FT and Oliveira PJ 2001, “Study of steady pipe and channel flows of a single-mode Phan-Thien—Tanner fluid”, J. Non-Newt. Fluid Mech., Vol. 101, pp. 55-76.

Bhatnagar RK 1963, “Steady laminar flow of visco-elastic fluid through a pipe and through an annulus with suction or injection at the walls”, J. Ind. Inst. Sci., Vol. 45, pp. 126-151.

Cruz DOA and Pinho FT 2004, “Skewed Poiseuille-Couette flows of SPTT fluids in concentric annuli and channels. J. Non-Newt. Fluid Mech., in press.

Dierckes AC and Schowalter WR 1966, “Helical flow of a non-Newtonian polyisobutelene solution”, Ind. Eng. Chem. Fund., Vol. 5, pp. 263-271.

Escudier MP, Oliveira PJ and Pinho FT 2002a, “Fully developed laminar flow of purely viscous non-Newtonian liquids through annuli, including the effects of eccentricity and inner-cylinder rotation”, Int.. J. Heat and Fluid Flow, Vol. 23, pp. 52-73.

Escudier MP, Oliveira PJ, Pinho FT and Smith S 2002b, “Fully developed laminar flow of non-Newtonian liquids through annuli: comparison of numerical calculations with experiments”, Exp. in Fluids, Vol. 33, pp. 101-111.

Kaloni PN 1965, “On the helical flow of an elasto-visccous fluid”, Ind. J. Pure Appl. Phys., Vol. 3, pp. 1-3.

Kulshrestha PK 1962, “Helical flow of an idealized elastico-viscous liquid (I)”. ZAMP, Vol. XIII, pp. 553-561.

Nouar C, Desaubry C and Zenaidi H 1998. “Numerical and experimental investigation of thermal convection for a thermodependent Herschel-Bulkley fluid in an annular duct with rotating inner cylinder”, Eur. J. Mech. B, Vol. 17, pp. 875-900.

Phan-Thien N and Tanner RI 1977, “A new constitutive equation derived from network theory”, J. Non-Newt. Fluid Mech., Vol. 2, pp. 353-365.

Pinho FT and Oliveira PJ 2000, “Axial annular flow of a non-linear viscoelastic fluid — an analytical solution”, J. Non-Newt. Fluid Mech., Vol. 93, pp. 325-337.